Pergamon

Available online at www.sciencedirect.com
SCIENCE DIRECT®

Cement and Concrete Research 33 (2003) 1515–1523

CEMENT AND CONCRETE RESEARCH

Natural 1.1 and 1.4 nm tobermorites from Fuka, Okayama, Japan: Chemical analysis, cell dimensions, ^{29}Si NMR and thermal behavior

Takayuki Maeshima[a,*], Hiroaki Noma[b], Masato Sakiyama[c], Takeshi Mitsuda[d]

[a]*A&A Material Corporation, 263-3 Uchiyodo, Akeno, Makabe, Ibaraki 300-4507, Japan*
[b]*AIST Kyushu, Institute for Structural and Engineering Materials, National Institute of Advanced Industrial Science and Technology (AIST), 807-1 Shuku, Tosu, Saga 841-0052, Japan*
[c]*A&A Material Corporation, 1-1 Tooyama, Kitasaki, Oobu, Aichi 474-0001, Japan*
[d]*Faculty of Engineering, East-Asia University, 2-1 Ichinomiyagakuen, Shimonoseki, Yamaguchi 751-8503, Japan*

Received 22 August 2002; accepted 20 March 2003

Abstract

A natural specimen of tobermorite, which contained both 1.1 and 1.4 nm phases, was studied by optical microscopy, X-ray powder diffractometry (XRD), EPMA, analytical TEM, ^{29}Si NMR and TG-DTA, and the results were compared with those for a specimen from Crestmore, California. The sample, occurring as a vein in contact with metamorphic rocks, could be divided into three zones. In two of the zones containing only the 1.1 nm phase, about 10% of the Si were substituted by Al. The third zone was an intergrowth of 1.1 and 1.4 nm tobermorites and contained almost no Al. The basal spacings of the 1.1 and 1.4 nm tobermorites were changed mainly to 0.9 nm by heating at 300 °C for 24 h but in some parts remained at 1.1 nm. ^{29}Si NMR results showed that silicate anions in the 1.1 nm tobermorite were double chains, which changed mainly into single chains, on heating at 300 °C. XRD results indicated that natural tobermorites are more highly crystalline than the synthetic ones of calcium silicate products.

Keywords: Tobermorite; Natural mineral; X-ray diffraction; Characterization; NMR

1. Introduction

Tobermorite is a main constituent of autoclaved calcium silicate products, such as sand–lime brick, autoclaved aerated concrete (AAC), thermal insulation board, fiber-reinforced calcium silicate sheets and other types of building materials. These products are made hydrothermally using silica with lime or cement under saturated steam pressure at 170–210 °C for 5–8 h. Tobermorite is also known as a natural mineral, first discovered by Heddle [1] in 1880 at Tobermory, Scotland. Taylor [2] and Claringbull and Hey [3] showed that natural tobermorite and "well-crystallized synthetic calcium silicate hydrate (I)" were essentially identical. Tobermorite has been studied using both natural and synthetic phases. Natural tobermorite is usually more highly crystalline than synthetic.

Tobermorites reported as natural minerals comprise the 1.4 nm ($Ca_5Si_6O_{18}H_2{\cdot}8H_2O$) [2,4–9], 1.1 nm ($Ca_5Si_6O_{17}{\cdot}5H_2O$) [3,5,8,10–12], 1.0 nm ($CaO{\cdot}0.1B_2O_3{\cdot}0.8SiO_2{\cdot}1.25H_2O$, oyelite) [2,13] and 0.9 nm ($Ca_5Si_6O_{18}H_2$) [5,14] phases, denoted from the value of the basal spacing, and clinotobermorite ($Ca_5Si_6O_{17}{\cdot}5H_2O$), which presents the same basal spacing as the 1.1 nm phase but displays a distinct diffraction pattern [15–17]. Tobermorite in autoclaved calcium silicate products has only been found as the 1.1 nm phase. Substitution of a part of the Si atoms in SiO_4 tetrahedra with Al is observed in natural and synthetic 1.1 nm tobermorites. The 1.4 nm tobermorite shows only a minor degree of Al substitution.

Megaw and Kelsey [18] and Hamid [19] determined the crystal structure of 1.1 nm tobermorite using natural single crystals. However, a clear and definite understanding of the complete structure was not obtained because of the stacking disorder [5,19]. The existence of double-chain silicate anions in 1.1 nm tobermorite was first proved by Wieker et al. [20] using ^{29}Si solid-state NMR spectroscopy. Subsequently, the results of many ^{29}Si NMR studies [20–28]

* Corresponding author. Tel.: +81-296-52-6521; fax: +81-296-52-6524.
E-mail address: maeshima@aamrc.jp (T. Maeshima).

0008-8846/03/$ – see front matter © 2003 Elsevier Ltd. All rights reserved.
doi:10.1016/S0008-8846(03)00099-1

showed that most of 1.1 nm tobermorite has double silicate chains formed by linking of bridging tetrahedra across the interlayer region, that the double-chain structure changes into a single-chain structure on heating at 300 °C and that the Al atom is selectively concentrated in the Q^3 sites.

Recently, Merlino et al. [17,29] determined the crystal structures of clinotobermorite and 1.1 and 0.9 nm tobermorites using X-ray single crystal technique with natural samples. The 1.1 nm tobermorite and clinotobermorite have layer structures. A unit layer is formed by a sevenfold-coordinated calcium polyhedral sheet, parallel to (001) and wollastonite-like silicate chains (called ''dreierketten,'' consisting of paired tetrahedra and bridging tetrahedra) running along the *b*-axis and attached on both sides of the calcium sheet. These chains connect adjacent unit layers and form a double-chain structure through the bridging oxygen. There are zeolitic Ca^{2+} ions and water molecules in channels between the unit layers. More recently, Merlino et al. [30] and Yamazaki and Toraya [31] succeeded in determining the positions of a zeolitic Ca^{2+} ion and three water molecules in a 1.1 nm tobermorite. Yamazaki and Toraya reported that the zeolitic Ca^{2+} site splits into two sites, each having 0.5 site occupancy, and that it is coordinated with three water molecules and three oxygen atoms. Merlino et al. suggested that two situations occur in these channels: the zeolitic Ca^{2+} is located in one case and absent in the other.

Whether natural or synthetic, 1.1 nm tobermorite generally occurs in two varieties, called normal and anomalous [12]. Upon heating to 300 °C, both varieties lose interlayer water; however, in the case of the normal type, the lattice shrinks from 1.1 to 0.9 nm. The anomalous variety does not shrink. Both normal and anomalous types change to wollastonite at about 850 °C. For the differences between normal and anomalous types, Mitsuda and Taylor [32] reported the following characteristics by examination of published data for natural tobermorite. Normal tobermorite had a higher Ca/(Al + Si) ratio and lower contents in Al and alkalis compared with the anomalous type, while the anomalous type has a lower Ca/(Al + Si) ratio and relatively higher contents of Al and alkalis. El-Hemaly et al. [33] reported that the hydrothermal formation of tobermorite proceeds through the sequence C-S-H → normal tobermorite → anomalous tobermorite → xonotlite. Merlino et al. [30] suggested that whether the tobermorite is normal or anomalous depends on the amount of zeolitic Ca^{2+}.

The 1.1 nm tobermorite has a wide range of Ca/(Al + Si) ratio. The Ca/(Al + Si) atomic ratio of natural tobermorite is generally in the range of 0.71–1.14 [32]. Mitsuda et al. [34] showed that tobermorites in calcium silicate products have a mean Ca/(Al + Si) atomic ratio of 0.76–1.09. Sakiyama et al. [24] indicated that the maximum substitution of Al/(Al + Si) is 0.13–0.14 in 1.1 nm tobermorite. At this ratio, the tobermorite coexisted with a trace of hydrogarnet, which was detected by electron microscopy for specimens prepared at a starting ratio of Al/(Al + Si) = 0.15. It was found that an increase in the substitution of Si by Al caused almost no change in the cell dimensions in the *a*- and *b*-axis but a large increase in the *c*-axis [24,35].

The 1.4 nm tobermorite occurs rarely as a natural mineral. The crystal structure of the 1.4 nm tobermorite is similar to that of 1.1 nm tobermorite with additional water molecules, but 1.4 nm tobermorite has a single-chain silicate anion structure [9]. Kalousek and Roy [36] first synthesized 1.4 nm tobermorite. They processed lime and silicic acid with a Ca/Si ratio = 1.0 at 60 °C for 6 months. Hara et al. [37,39] and Hara and Inoue [38,40] obtained 1.4 nm tobermorite by processing for 10–20 days at 80–90 °C using lime and amorphous silica (such as silica glass, fumed silica and rice husk ash) with starting Ca/Si ratios of 0.6–0.9. However, using similar conditions, 1.4 nm tobermorite could not be synthesized from starting materials containing Al. They suggested that 1.4 nm tobermorite is a stable phase at reaction temperatures less than 80 °C in the absence of Al. The Ca/Si ratio of 1.4 nm tobermorite is higher than that of 1.1 nm tobermorite [32].

In this paper, some mineralogical properties of natural tobermorites, including mixtures of the 1.1 and 1.4 nm phases from Fuka, were investigated using optical microscopy, X-ray powder diffractometry (XRD), ^{29}Si solid-state NMR spectroscopy, thermal analysis and chemical analysis. The formation of natural tobermorites is compared with that of synthetic ones in calcium silicate products.

2. Experimental procedure

2.1. Materials

The 1.1 and 1.4 nm tobermorite samples were obtained from Fuka, Okayama, Japan. The geology of this area is composed of Paleozoic limestone, lutite, chert and contact metamorphic rocks of these with intrusive igneous rocks. Fuka, where all phases of the tobermorite group except 0.9 nm phase occur, is one of the most important localities for tobermorites, being equal to Crestmore. This sample occurred in a vein of approximately 10 mm width within the altered rock, which is mainly composed of alkali feldspar and pyroxene. The sample is strongly consolidated and has a color of white or milky white. This sample was kindly provided by Prof. I. Kusachi, Okayama University. The main characteristics of this sample have been reported by Mitsuda et al. [8]. The present study is a more detailed reexamination of the same sample. The 1.4 nm tobermorite from Crestmore, California, kindly provided by Prof. H.F.W. Taylor, was used as a reference material. Moreover, we also used autoclaved calcium silicate products such as sand–lime brick, AAC and thermal insulation board.

2.2. Experimental methods

The crystal morphology and texture of the 1.1 and 1.4 nm tobermorites from Fuka were observed with an optical

microscope. Crystal phases, crystallite sizes and cell dimensions of the samples were examined by XRD (XD-D1, Shimazu) using graphite-monochromatized Cu $K\alpha$ radiation with a step scan method: step width = 0.02°, conducting each step for 4 s. The 002, 220 and 222 reflections for tobermorites were used for the calculation of the crystallite size. In order to correct for instrumental line broadening, a quartz grain with 25–55 μm across, heated at 800 °C for 24 h, was used as the standard. The subcell dimensions of 1.1 and 1.4 nm tobermorites were determined by a least-squares refinement of 8–18 reflections. Computations were conducted using a space group of 12 mm for both 1.1 and 1.4 nm tobermorite and the subcell was given by Merlino et al. [9,29] as the initial values.

The Ca/(Al + Si) and Al/(Al + Si) ratios and the potassium contents of the natural tobermorites were obtained using EPMA (JXA-8621M, JEOL), SEM-EDS (ALPHA-30A, Akashi with EDS) and analytical electron microscopy (ATEM; JEM-2000 FX, JEOL, with EDS). The standard materials used for EPMA were aluminum oxide (Al_2O_3) for Al, wollastonite ($CaSiO_3$) for Ca and Si and adularia (a K-feldspar) for K. Counting times were 10 s. The accelerating voltage was 15 kV, and the sample current was 30 nA. Analyzing conditions for the SEM-EDS are as follows: 20 kV acceleration voltage, 1 nA sample current (on MgO), 30° tilt angle, 30 mm working distance and 100 s integration time. For ATEM, natural xonotlite and natural kaolinite were used as the standards to confirm the K factor of Ca/Si and Al/Si ratios, respectively.

To examine the silicate anion structure of tobermorite, ^{29}Si solid-state NMR spectra were recorded on a Bruker DSX300WB at 59.6 MHz by high-power decoupling (HD) or cross polarization (CP) with magic angle spinning (MAS) of 5 kHz. HD-MAS spectra were acquired with a repetition time of 240 s, the use of π/4 pulses (2.75 μs) and an accumulation number of 512. For CP-MAS spectra, the repetition time, the contact time and the accumulation number were 10 s, 2 ms and 1024, respectively. The standard material used was 3-(trimethylsilyl)-propane sulfonic acid sodium salt (DSS) and its ^{29}Si chemical shift was 1.534 ppm [42]. The TG-DTA curves were simultaneously recorded by heating about 30 mg of the sample from Fuka with a heating rate of 10 °C/min using a Rigaku TAS300 thermal analysis system. The samples after heating at 300 °C for 20 h were also examined by NMR and XRD to determine their structural change.

3. Results and discussion

3.1. Optical micrographs

Fig. 1 shows the optical micrographs of the vein of 1.1 and 1.4 nm tobermorites. This sample has a zone structure parallel to the vein elongation, symmetrically centered to the outside. Mitsuda et al. [8] reported that three zones could be distinguished in this white vein: the central part being of 1.1 nm tobermorite, surrounded by an intergrowth of 1.1 and 1.4 nm tobermorites and the outer layers being of 1.1 nm tobermorite in contact with the altered rock. Correspondingly, we separately named the zones A, B and C in order from the center to the outside, and the C zone was divided into subzones of C1 and C2.

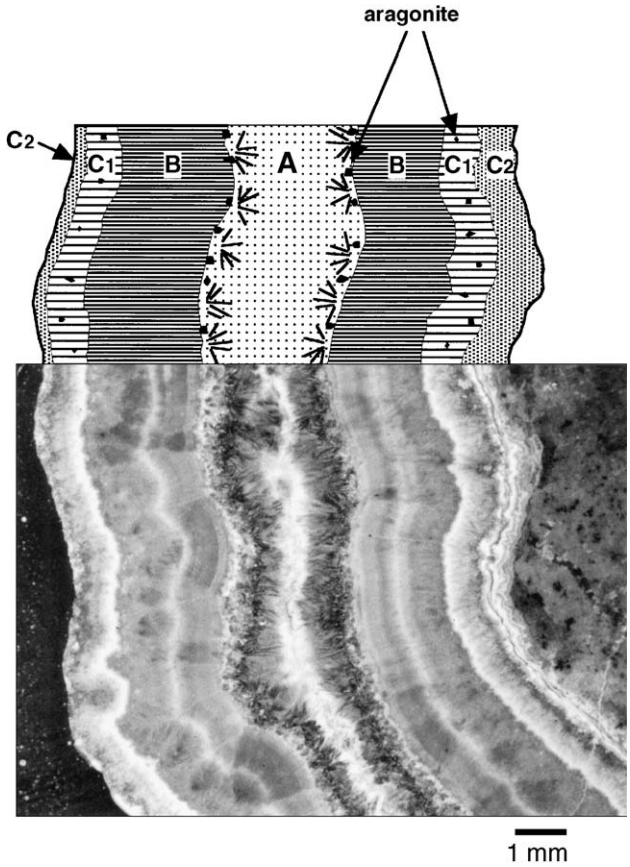

Fig. 1. Optical micrographs for the 1.1 and 1.4 nm tobermorites from Fuka. A: 1.1 nm tobermorite zone, B: intergrowth zone of 1.1 and 1.4 nm tobermorites and C: 1.1 nm tobermorite zone.

The A zone is composed of large needle-like and/or plate-like crystals, growing radially towards the center, and relatively large crystals with smaller ones between them. In the B zone, small crystals having fiber-like morphology grow vertically with respect to the vein elongation. The C zone is dense with small crystals. Aragonite was detected at the boundary of the A and B zones and also in the C1 zone.

3.2. XRD result

Fig. 2 shows XRD patterns for the 1.1 and 1.4 nm tobermorites of the whole vein without separating the zones of the Fuka material and for the 1.4 nm tobermorite from Crestmore before and after being heated at 300 °C for 20 h. Both of the samples without heating are highly crystalline. The sample from Fuka was confirmed to consist of mixtures

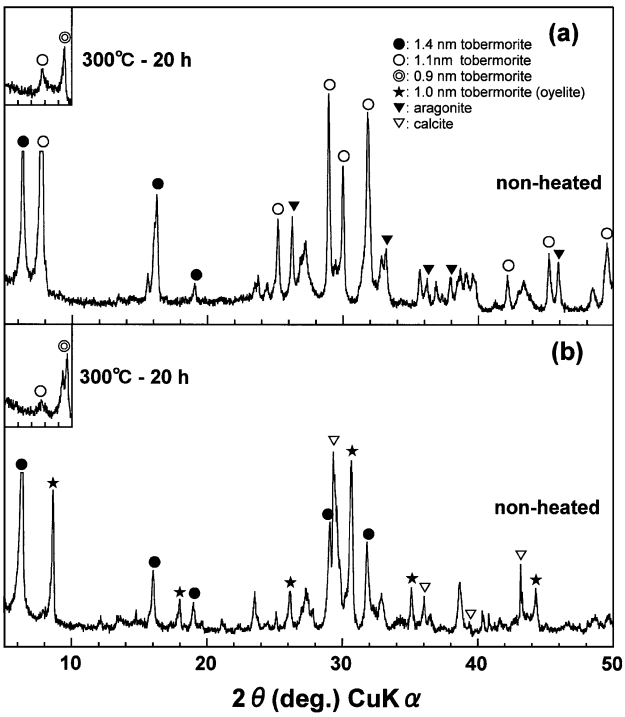

Fig. 2. XRD patterns for the tobermorites from (a) Fuka, the whole vein without separating the zones, and (b) Crestmore before and after being heated at 300 °C for 20 h.

of 1.1 and 1.4 nm tobermorites with a small amount of aragonite. The stronger basal reflection of 1.1 nm tobermorite indicates that this sample is enriched in 1.1 nm tobermorite. The sample from Crestmore is mainly composed of 1.4 nm tobermorite with some 1.0 nm tobermorite (oyelite) and calcite.

Fig. 3 shows XRD patterns for zones A, B and C before and after being heated at 300 °C for 20 h. It was confirmed that the A and C zones contain only 1.1 nm tobermorite and that a mixture of 1.1 and 1.4 nm tobermorites occurs only in the B zone. In addition, the B zone is enriched in 1.4 nm tobermorite. The relatively high diffracted intensity between 1.1 and 1.4 nm peaks suggests that a phase of intermediate spacing [39–41] or C-S-H (I) is also present.

3.3. Chemical compositions

Table 1 gives Ca/(Al + Si) and Al/(Al + Si) ratios and K_2O contents (mass %) calculated from the EPMA, SEM-EDS and ATEM results. The Ca/(Al + Si) ratios of the tobermorite in the A, C1 and C2 zones, containing only the 1.1 nm phase, are 0.78, 0.79 and 0.78, respectively, being slightly lower than the ideal value, 0.83 for tobermorite, while the ratio in the B zone rich in 1.4 nm tobermorite equals the ideal value. The Al/(Al + Si) ratio is about 0.10 in the A and C1 zones, and the ratio in the C2 zone is 0.13, which is almost the limiting value of Al substitution in tobermorite [24]. On the other hand, tobermorites in the B zone contain very little Al. The potassium content is relatively high in the A, C1 and C2 zones but was hardly detectable in the B zone.

The 1.4 nm tobermorite from Crestmore contained no Al and had a relatively high Ca/(Al + Si) ratio. This result is similar to that found for the B zone containing the 1.1 and 1.4 nm tobermorites and agrees well with those for 1.4 nm tobermorite reported by Mitsuda and Taylor [32].

3.4. Subcell dimensions

Table 2 gives subcell dimensions for the 1.1 and 1.4 nm tobermorites in the A, B and C zones from Fuka and for the 1.4 nm tobermorite from Crestmore. The 1.1 nm tobermorite in the B zone with a low Al content has $a = 0.5629(6)$ nm, $b = 0.3683(10)$ nm and $c = 2.249(5)$ nm, which closely agrees with the results for a synthetic Al-free tobermorite ($a = 0.5622(3)$ nm, $b = 0.3691(3)$ nm, and $c = 2.247(2)$ nm) reported by Sakiyama et al. [24]. On the other hand, the subcell dimensions of those in the A and C zones are similar to the results for the Al tobermorite [24] ($a = 0.5625(2)$ nm, $b = 0.3688(1)$ nm and $c = 2.267(6)$ nm) prepared from lime–quartz mixtures with an Al/(Al + Si) ratio of 0.10. Increasing the Al/(Al + Si) ratio in tobermorite caused almost no change in the *a*- and *b*-axis but greatly elongated the *c*-axis. The 1.4 nm tobermorite in the B zone has the subcell dimensions $a = 0.5632(7)$ nm, $b = 0.3677(5)$ nm and $c = 2.791(5)$ nm, which are analogous to those of 1.4 nm tobermorite from Crestmore or the single crystal results ($a = 0.563$ nm, $b = 0.364$ nm and $c = 2.796$ nm) reported by Merlino et al. [9].

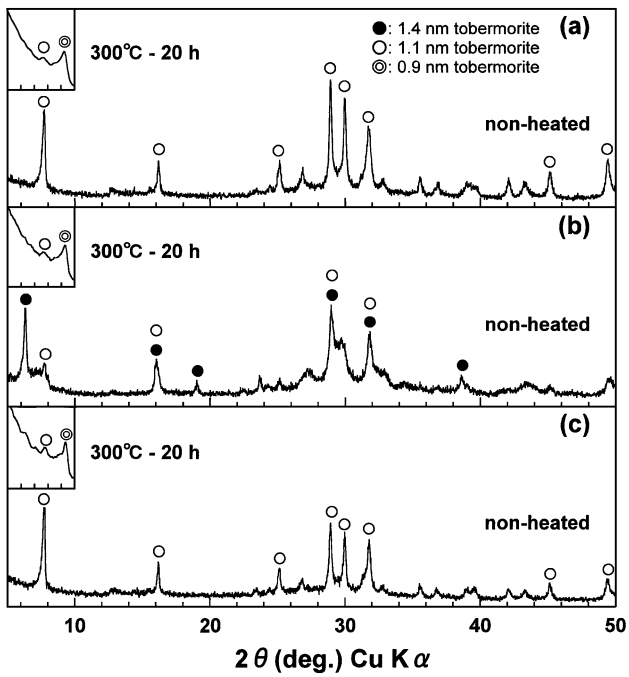

Fig. 3. XRD patterns for the A (a), B (b) and C (c) zones of tobermorite from Fuka before and after being heated at 300 °C for 20 h.

Table 1
Results of chemical analysis for tobermorite

Materials		Number of analyses	Atomic ratios								
			Ca/(Al+Si)			Al/(Al+Si)			K_2O (mass %)		
			Mean	Range	S.D.	Mean	Range	S.D.	Mean	Range	S.D.
Fuka[a]	A zone	13	0.78	0.75–0.82	0.02	0.09	0.06–0.11	0.01	0.25	0.16–0.36	0.05
	B zone	22	0.83	0.81–0.84	0.01	0.02	0.01–0.03	0.01	0.04	0.00–0.10	0.02
	C1 zone	20	0.79	0.77–0.82	0.01	0.09	0.06–0.11	0.01	0.24	0.19–0.33	0.03
	C2 zone	15	0.78	0.75–0.80	0.01	0.13	0.11–0.15	0.01	0.12	0.03–0.17	0.04
Crestmore[b]		28	0.85	0.80–0.91	0.03	0.00	0.00–0.02	0.01	–	–	–

[a] Results of EPMA and SEM-EDS.
[b] Results of ATEM.

3.5. Crystallite size

Table 3 gives the crystallite sizes for the natural tobermorites and synthetic ones in various autoclaved calcium silicate products. The crystallite sizes of the natural tobermorites are in the range of 56–123 nm in the [001] direction. The crystallite sizes in the [110] and [111] directions range from 63 to 343 nm. The results show that the crystallite morphology of the natural tobermorites is platy.

The crystallite sizes of the synthetic tobermorite in calcium silicate products are in the range of 16–28 nm in the [001] direction and are thinner than those of the natural ones. These values are similar to those of tobermorite in AAC reported by Isu et al. [43]. In the [001] and [110] directions, the crystallite sizes are larger than those of [001] direction and vary from 30 to 110 nm with the kind of products. The sand–lime brick is the same value in both [001] and [110] directions, while the crystallite of tobermorite in an AAC has high prevalence parallel to (001).

Autoclaved products are normally treated at 170–210 °C for tobermorite materials in order to shorten the autoclaving time. In this case, a 1.1 nm tobermorite is unstable and will certainly be changed into xonotlite during a long treatment time. Tobermorite is stable at 140 °C or lower temperatures. For this reason, natural tobermorites must be formed under the more stable conditions for tobermorites through the passage of a much longer time than autoclaved products. The difference in crystal growth process may appear in crystallite size. Therefore, compared with tobermorite of autoclaved products, natural crystals have a higher crystallinity, particularly in the [001] direction.

Table 2
Subcell dimensions of 1.1 and 1.4 nm tobermorites

Sample		Tobermorite (nm)	*a* (nm)	*b* (nm)	*c* (nm)	Volume (nm^3)
Fuka	A zone	1.1	0.5622(3)	0.3680(4)	2.272(2)	0.470
	B zone	1.4	0.5632(7)	0.3677(5)	2.791(5)	0.578
		1.1	0.5629(6)	0.3683(10)	2.249(5)	0.466
	C zone	1.1	0.5628(3)	0.3682(4)	2.264(2)	0.469
Crestmore		1.4	0.5634(8)	0.3663(6)	2.799(3)	0.578

3.6. NMR results

The silicate anion structures of the tobermorites were examined using ^{29}Si solid-state NMR. Fig. 4 shows the ^{29}Si HD-MAS and CP-MAS NMR spectra of the natural tobermorites. For the 1.1 and 1.4 nm tobermorites, the specimen used was the entire vein sample, without separating the A, B and C zones. The interpretation of ^{29}Si NMR spectra is based on that of Wieker et al. [20]. In the HD-MAS spectra for the 1.1 and 1.4 nm tobermorites, the signals correspond to chain middle groups Q^2 (−80.5 and −85.3 ppm) and branching sites Q^3 (−91.9 and −96.1 ppm). The result shows that this sample contains a double-chain structure of silicate anions, which agrees with the results of the previous NMR observations on 1.1 nm tobermorites [20,21,24] and with the crystal structure reported by Merlino et al. [29,30]. The signals at −80.5 and −91.9 ppm can be assigned to the Q^2(1Al) and Q^3(1Al) signals shifted to higher frequency by the Al substitution [21]. These chemical shifts are due to Al-substituted 1.1 nm tobermorite in the A and C zones. The signal at −83.8 ppm can be assigned to bridging Q^2 sites [27]. The enhancement of this signal by CP also suggests

Table 3
Crystallite size of tobermorites in natural materials and calcium silicate products

Materials		Crystallite size (nm)		
		[001]	[110]	[111]
Natural materials				
Fuka	A zone	123	343	192
	B zone	59[a]	–	–
	C zone	56	92	74
Crestmore		69[a]	63[a]	–
Calcium silicate products				
AAC		20	111	45
		21	103	48
Sand–lime brick		28	31	–
		21	36	–
		21	32	26
Calcium silicate board		19	50	37
		19	51	37
Thermal insulation		16	58	19

[a] Crystallite size for 1.4 nm tobermorite.

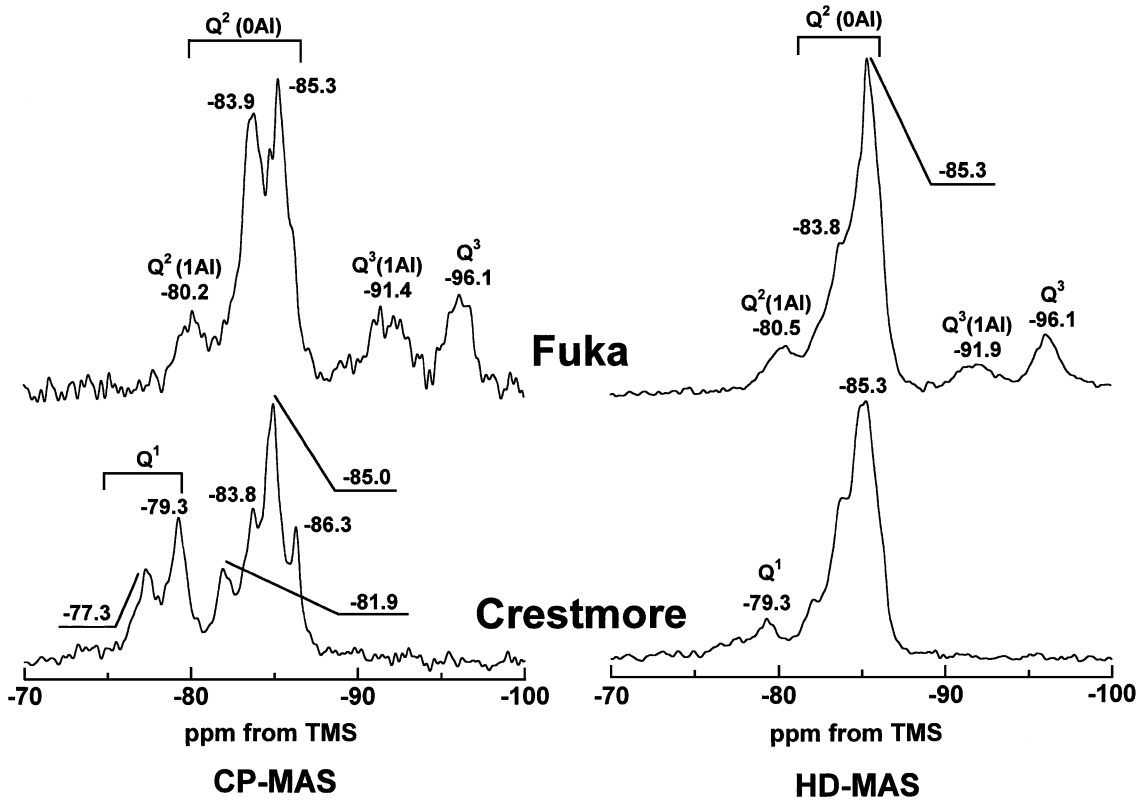

Fig. 4. ^{29}Si HD-MAS (left) and CP-MAS (right) NMR spectra for the 1.1 and 1.4 nm tobermorites from Fuka and the 1.4 nm tobermorite from Crestmore.

that some of the bridging Q^2 sites are protonated [27]. This result agrees with the crystal structure refined by Merlino et al. [29], who reported that some oxygen atoms in the tetrahedral chain can be replaced by hydroxyl groups.

The Crestmore 1.4 nm tobermorite gives mainly two signals at −85.3 and −79.3 ppm in HD-MAS. The signal at −85.3 ppm can be assigned to a Q^2 site. No Q^3 signal is observed. It is clear that 1.4 nm tobermorite has a single-chain structure. It is considered that the peak at −79.3 ppm is the Q^1 signal that indicates the end group of a chain structure or a dimer [20,26]. Since the Q^1 signal in CP-MAS spectra is relatively higher than that in the HD-MAS spectra, the Q^1 sites may be protonated. The other signals at −77.3, −81.9, −83.8 and −86.3 ppm are observed clearly in CP-MAS spectra. The signal at −77.3 ppm and the other three signals can be assigned to Q^1 and Q^2, respectively. It is not clear whether these signals, including that at −79.3 ppm, are due to either 1.4 nm tobermorite or oyelite. Taylor (private communication) suggested that oyelite has a tobermorite-like structure with the bridging tetrahedra either missing or replaced by borate groups. These signals may be assigned to dimers (Q^1) or to Q^2 sites affected by BO_4 in oyelite.

3.7. Thermal behavior

Fig. 5 shows the TG-DTA curve of the 1.1 and 1.4 nm tobermorites. The specimen is a portion of the vein, without separating the A, B and C zones. The DTA curve shows two strong endothermic peaks at about 105 and 234 °C. The first peak is attributable to the dehydration from 1.4 to 1.1 nm tobermorite and the second peak corresponds to the dehydration from the 1.1 nm to the 0.9 nm phase. An exothermic peak is clear at 847 °C, corresponding to the recrystallization into wollastonite. The TG curve shows a sharp loss to 300 °C and a more gradual one above 300 °C.

After heating at 300 °C for 24 h, the basal spacings of 1.1 and 1.4 nm for the Fuka sample (Figs. 2 and 3) shifted mainly to a 0.9 nm peak and a weak 1.1 nm peak remained

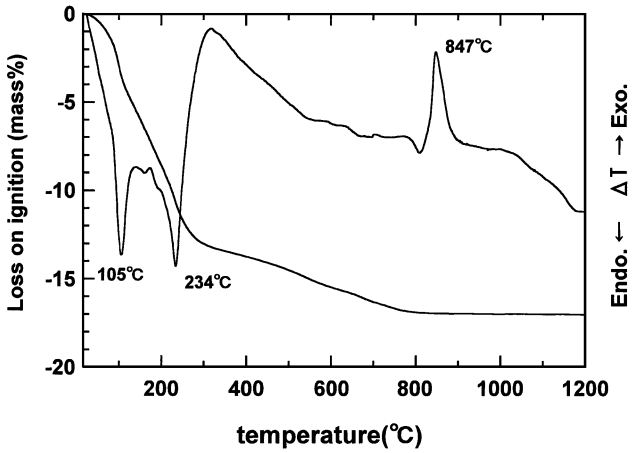

Fig. 5. TG-DTA curves for the 1.1 and 1.4 nm tobermorites from Fuka; whole vein without separating the zones.

for all the zones. The results show that both 1.4 and 1.1 nm tobermorites are mainly of normal type with some anomalous type. However, for the heated sample, the boundary between the 002 reflections of the 0.9 and 1.1 nm phases is not clear, which suggests the existence of the intermediate spacing or mixed-layer phase of 0.9 and 1.1 nm tobermorites [37,40] after dehydration of the interlayer water.

Fig. 6 shows the ^{29}Si NMR results for the samples after being heated at 300 °C for 20 h. For the 1.1 and 1.4 nm tobermorites, the Q^3 signal almost disappeared and only a broad Q^2 signal is observed. It is clear that the double-chain structure of the silicate anions for the 1.1 and 1.4 nm tobermorites was destroyed and converted into the single-chain structure. Compared with the nonheated sample, the Q^2 signal shifts to higher frequency from −85 to −83 ppm and becomes much broader, and the signal of CP-MAS is considerably enhanced. The change from the double chains to the single chains causes a conversion from the Q^3 sites to the bridging Q^2 sites, and the broken Si-O-Si bonds must produce much Si-OH. The chemical shifts of the bridging Q^2 sites of tobermorites are around −85.3 ppm, as shown in Fig. 4, and those of protonated bridging Q^2 are around −83.8 ppm, which explains why the Q^2 signal shifts to a higher frequency. The broadening of the signal is mainly due to the distortion of the structure caused by heating.

As shown in Fig. 2, the Crestmore 1.4 nm tobermorite also showed mixed thermal behavior on heating at 300 °C and the 1.0 nm tobermorite disappears. Figs. 4 and 6 show that the Crestmore 1.4 nm tobermorite maintains a single-chain structure before and after heating. After heating, various Q^2 signals are observed. They comprise sharp peaks at −85.0 and −86.4 ppm in the HD-MAS spectrum and a broad peak at −83.2 ppm with subsidiary peaks at −84.6 and −86.3 ppm in the CP-MAS spectrum. As with the Fuka sample, the broad peak at −83.2 ppm can be assigned to protonated Q^2 in 0.9 nm tobermorite.

3.8. Tobermorite formation

Since the composition of each zone is almost uniform and the boundaries between zones are clear from the results of the microscope observation, XRD and composition analysis, indications are that the solution that flowed into the crack in the host rock differs in each zone. It is thought that the sample from Fuka was formed toward the inside from the outside. At first, the solution that is rich in Al content flowed into the crack, and C zone was formed. Next, B zone, mainly consisting of 1.4 nm tobermorite, was formed from the solution with poor Al content, and A zone was formed from the Al-rich solution again. The stability

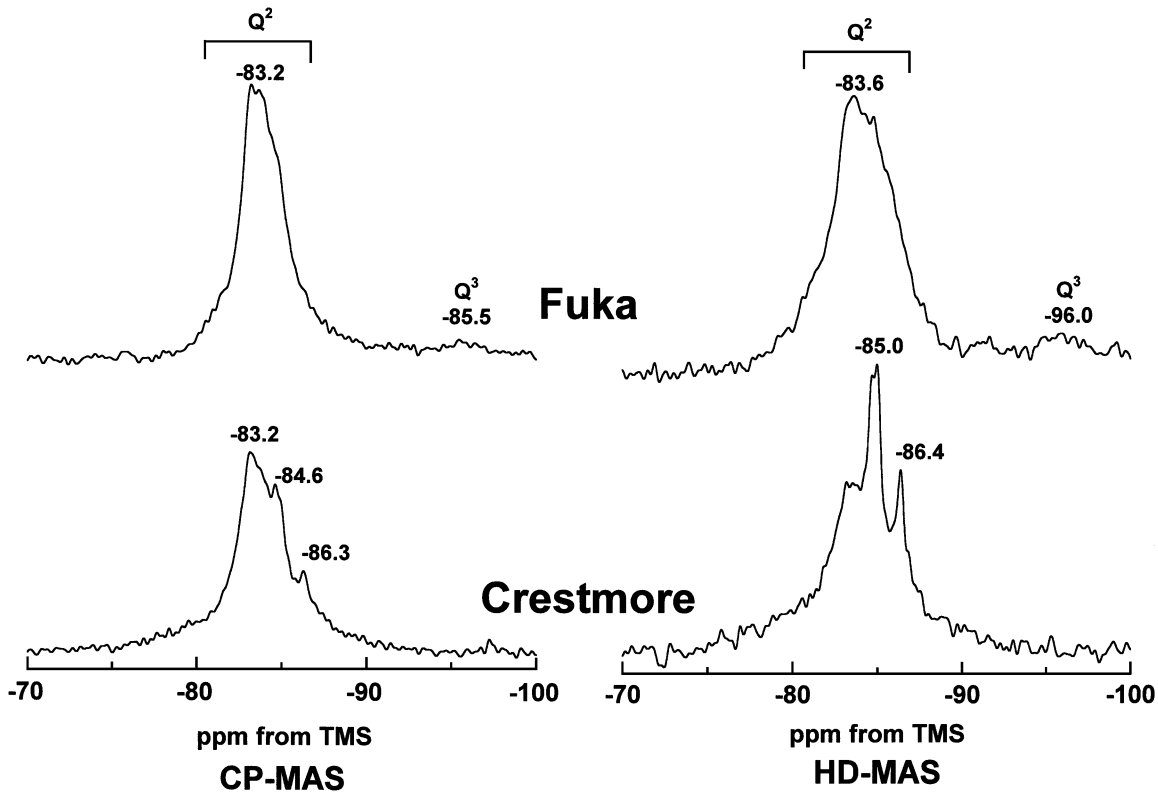

Fig. 6. ^{29}Si HD-MAS (left) and CP-MAS (right) NMR spectra for the 1.1 and 1.4 nm tobermorites from Fuka and the 1.4 nm tobermorite from Crestmore after being heated at 300 °C for 20 h.

boundary for the 1.4 and 1.1 nm phases without Al might be near 60 °C, and when Al content is included, it might be at an even lower temperature [36,37,39]. Therefore, in the Fuka field, the temperature of the formation of the vein formed might have been 60 °C or less.

4. Conclusions

(1) The 1.1 and 1.4 nm tobermorites from Fuka in Japan occurred as a vein 10 mm in width within altered rock, containing a small amount of aragonite. This tobermorite vein was probably formed from calcium silicate solutions with and almost without Al at a low temperature near 60 °C. The vein is composed, from the center to the side, of a 1.1 nm tobermorite zone, an intergrowth zone of 1.1 and 1.4 nm tobermorites and a 1.1 nm tobermorite zone.
(2) The intergrowth zone of 1.1 and 1.4 nm tobermorites contains almost no Al, having a Ca/(Al + Si) atomic ratio of 0.82, while in the central and the outermost zones the Al/(Al + Si) and Ca/(Al + Si) atomic ratios of the 1.1 nm tobermorite are about 0.10 and 0.78, respectively.
(3) The 1.4 nm tobermorite has a single-chain silicate anion, while 1.1 nm tobermorite has a double-chain silicate anion that changes mainly into a single-chain structure on heating at 300 °C.
(4) The crystals of natural tobermorites are thicker, particularly in the [001] direction, than those of tobermorites in calcium silicate products.

Acknowledgements

The authors are grateful to Prof. I. Kusachi, Okayama University, for providing the Fuka sample and to Prof. H.F.W. Taylor, for providing the Crestmore sample and for his valuable comments on this work. The authors also wish to thank Dr. Y. Okada for obtaining the EPMA data, Dr. S. Yamazaki, INAX, for obtaining the TG-DTA data and Mr. D. Saito, Kanazawa University, for obtaining the SEM-EDS data.

References

[1] M.F. Heddle, Preliminary notice of substances which may prove to be new minerals, Mineral. Mag. 4 (1880) 117–123.
[2] H.F.W. Taylor, Crestmoreite and riversideite, Mineral. Mag. 30 (1953) 155–165.
[3] G.F. Claringbull, M.H. Hey, A re-examination of tobermorite, Mineral. Mag. 29 (1952) 960–962.
[4] J. Murdoch, Crestmore, past and present, Am. Mineral. 46 (1961) 245–257.
[5] J.D.C. McConnell, The hydrated calcium silicates riversideite, tobermorite, and plombierite, Mineral. Mag. 30 (1954) 293–305.
[6] V.C. Farmer, J. Jeevaratnam, K. Speakman, H.F.W. Taylor, Thermal decomposition of 14 Å tobermorite from Crestmore, Symp. Struct. Portland Cem. Paste Concr. Spec. Rep. 90, U.S. Highway Res. Board, Washington, 1966, pp. 291–299.
[7] J.D. Stephens, E. Bray, Occurrence and infrared analysis of unusual zeolitic minerals from Bingham, Utah, Mineral. Rec. 4 (1973) 67–72.
[8] T. Mitsuda, I. Kusachi, K. Henmi, Mixtures of 14 Å and 11 Å tobermorite from Fuka, Japan, Cem. Assoc. Jpn. Rev. Gen. Meet. 26 (1972) 64–68 (in Japanese).
[9] S. Merlino, E. Bonaccorsi, A.R. Kampf, Tobermorite 14 Å: crystal structure and OD character, in: D. Rammlmair, J. Mederer, Th. Oberthür, R.B. Heimann, H. Pentinghaus (Eds.), Applied Mineralogy, vol. 2, A.A. Balkema, Rotterdam, 2000, pp. 859–861.
[10] T. Mitsuda, Paragenesis of 11 Å tobermorite and poorly crystalline hydrated magnesium silicate, Cem. Concr. Res. 3 (1973) 71–80.
[11] J.M. Sweet, Tacharanite and other hydrated calcium silicates from Portree, Isle of Skye, Mineral. Mag. 32 (1961) 745–753.
[12] J.A. Gard, H.F.W. Taylor, A further investigation of tobermorite from Loch Eynort Scotland, Mineral. Mag. 31 (1957) 361–370.
[13] I. Kusachi, C. Henmi, K. Henmi, An oyelite-bearing vein at Fuka, the town of Bitchu, Okayama Prefecture, J. Jpn. Assoc. Miner. Petrol. Econ. Geol. 79 (1984) 267–275.
[14] L. Heller, H.F.W. Taylor, Crystallographic Data for the Calcium Silicates, HMSO, London, 1956, pp. 37–38.
[15] C. Henmi, I. Kusachi, Clinotobermorite, $Ca_5Si_6(O,OH)_{18}\cdot 5H_2O$, a new mineral from Fuka, Okayama Prefecture, Japan, Mineral. Mag. 56 (1992) 353–358.
[16] C. Hoffmann, T. Armbruster, Clinotobermorite, $Ca_5[Si_3O_8(OH)]_2\cdot 4H_2O$-$Ca_5[Si_6O_{17}]\cdot 5H_2O$, a natural C-S-H (I) type cement mineral: determination of the substructure, Z. Kristallogr. 212 (1997) 864–873.
[17] S. Merlino, E. Bonaccorsi, T. Armbruster, The real structures of clinotobermorite and tobermorite 9: OD character, polytypes, and structural relationships, Eur. J. Mineral. 12 (2000) 411–429.
[18] H.D. Megaw, C.H. Kelsey, Crystal structure of tobermorite, Nature 177 (1956) 390–391.
[19] S.A. Hamid, The crystal structure of the 11 Å natural tobermorite $Ca_{2.25}[Si_3O_{7.5}(OH_{1.5})]\cdot 1H_2O$, Z. Kristallogr. 154 (1981) 189–198.
[20] W. Wieker, A.T. Grimmer, A. Winkler, M. Magi, M. Tarmak, E. Lippmaa, Solid-state high-resolution ^{29}Si NMR spectroscopy of synthetic 14 Å, 11 Å, and 9 Å tobermorite, Cem. Concr. Res. 12 (1982) 333–339.
[21] S. Komarneni, R. Roy, D.M. Roy, C.A. Fyfe, G.J. Kennedy, A.A. Bothner-By, J. Dadok, A.S. Chesnick, ^{27}Al and ^{29}Si magic angle spinning nuclear magnetic resonance spectroscopy of Al-substituted tobermorites, J. Mater. Sci. 20 (1985) 4209–4214.
[22] S. Komarneni, D.M. Roy, C.A. Fyfe, G.J. Kennedy, Naturally occurring 1.4 nm tobermorite and synthetic jennite: characterization by ^{27}Al and ^{29}Si MASNMR spectroscopy and cation exchange properties, Cem. Concr. Res. 17 (1987) 891–895.
[23] X. Cong, R.J. Kirkpatrick, ^{29}Si and ^{17}O NMR investigation of the structure of some crystalline calcium silicate hydrates, Adv. Cem. Based Mater. 3 (1996) 133–143.
[24] M. Sakiyama, T. Maeshima, T. Mitsuda, Synthesis and crystal chemistry of Al-substituted 11 Å tobermorite, J. Soc. Inorg. Mater. Jpn. 7 (2000) 413–419.
[25] M. Tsuji, S. Komarneni, P. Malla, Substituted tobermorites: ^{27}Al and ^{29}Si MASNMR, cation exchange, and water sorption studies, J. Am. Ceram. Soc. 74 (1991) 274–279.
[26] Y. Okada, H. Ishida, T. Mitsuda, ^{29}Si NMR spectroscopy of silicate anions in hydrothermally formed C-S-H, J. Am. Ceram. Soc. 77 (1994) 765–768.
[27] H. Noma, Y. Adachi, H. Yamada, T. Nishino, Y. Matsuda, T. Yoko- yama, ^{29}Si MAS NMR spectroscopy of poorly-crystalline calcium silicate hydrate (C-S-H), in: P. Colombet, A.-R. Zanni, H. Zanni, P. Sozzani (Eds.), Nuclear Magnetic Resonance Spectroscopy of Cement-Based Materials, Springer-Verlag, Berlin, 1998, pp. 159–168.
[28] T. Mitsuda, H. Toraya, Y. Okada, M. Shimoda, Synthesis of to-

bermorite: NMR spectroscopy and analytical electron microscopy, in: W.S. Young, G.L. Mcvay, G.E. Pike (Eds.), Ceramic Transactions, vol. 5, Am. Ceram. Soc., Ohio, 1989, pp. 206–213.
[29] S. Merlino, E. Bonaccorsi, T. Armbruster, Tobermorites: their real structure and order–disorder (OD) character, Am. Mineral. 84 (1999) 1613–1621.
[30] S. Merlino, E. Bonaccorsi, T. Armbruster, The real structure of tobermorite 11 Å: normal and anomalous forms, OD character and polytypic modifications, Eur. J. Mineral. 13 (2001) 577–590.
[31] S. Yamazaki, H. Toraya, Determination of positions of zeolitic calcium atoms and water molecules in hydrothermally formed aluminum-substituted tobermorite-1.1 nm using synchrotron radiation powder diffraction data, J. Am. Ceram. Soc. 84 (11) (2001) 2685–2690.
[32] T. Mitsuda, H.F.W. Taylor, Normal and anomalous obermorites, Mineral. Mag. 42 (1978) 229–235.
[33] S.A.S. El-Hemaly, T. Mitsuda, H.F.W. Taylor, Synthesis of normal and anomalous tobermorites, Cem. Concr. Res. 7 (1977) 429–438.
[34] T. Mitsuda, K. Sasaki, H. Ishida, Phase evolution during autoclaving process of aerated concrete, J. Am. Ceram. Soc. 75 (1992) 1858–1863.
[35] N. Hara, N. Inoue, Thermal behaviour of 11 Å tobermorite and its lattice parameters, Cem. Concr. Res. 10 (1980) 53–60.
[36] G.L. Kalousek, R. Roy, Crystal chemistry of hydrous calcium silicates: II. Characterization of interlayer water, J. Am. Ceram. Soc. 40 (1957) 236–239.
[37] N. Hara, C.F. Chan, T. Mitsuda, Formation of 14 Å tobermorite, Cem. Concr. Res. 8 (1978) 113–116.
[38] N. Hara, N. Inoue, Formation of 14 Å tobermorite from silica glass, Ceram. Soc. Jpn. 84 (1976) 181–185 (in Japanese).
[39] N. Hara, N. Inoue, H. Noma, Formation of jennite and tobermorite and their relationship with C-S-H gel in hydrated cement paste, in: M. Cohen, S, Mindess, J. Skalny (Eds.), Materials Science of Concrete—The Sydney Diamond Symposium, The American Ceramic Society, Westerville (Ohio, USA), 1998, pp. 71–80.
[40] N. Hara, N. Inoue, Hydrothermal reaction of silica glass with lime at 70°–100 °C, Ceram. Soc. Jpn. 87 (1979) 134–141 (in Japanese).
[41] P. Yu, R.J. Kirkpatrick, Thermal dehydration of tobermorite and jennite, Concr. Sci. Eng. 1 (1999) 185–191.
[42] S. Hayashi, K. Hayamizu, Chemical shift standards in high-resolution solid-state NMR (1) ^{13}C, ^{29}Si, and ^{1}H nuclei, Bull. Chem. Soc. Jpn. 64 (1991) 685–687.
[43] N. Isu, K. Sasaki, H. Ishida, T. Mitsuda, Mechanical property evolution during autoclaving process of aerated concrete using slag: I. Tobermorite formation and reaction behavior of slag, J. Am. Ceram. Soc. 77 (1994) 2088–2092.